

Retrospective Synthetic Focusing with Correlation Weighting for Very High Frame Rate Ultrasound

Chang-Lin Hu, Yao-You Cheng, and Meng-Lin Li

Abstract—The need of high frame-rate imaging has been triggered by the new applications of ultrasound imaging to transient elastography and real-time 3D ultrasound. Using plane wave excitation (PWE) is one of the methods to achieve very high frame-rate imaging since an image can be formed with a single insonification. However, due to the lack of transmit focusing, the image quality with PWE is lower compared with those using conventional focused transmission. To solve this problem, we propose a filter-retrieved transmit focusing (FRF) technique combined with cross-correlation weighting (FRF+CC weighting) for high frame-rate imaging with PWE. A retrospective focusing filter is designed to simultaneously minimize the predefined sidelobe energy associated with single PWE and the filter energy related to the signal-to-noise-ratio (SNR). This filter attempts to maintain the mainlobe signals and to reduce the sidelobe ones, which gives similar mainlobe signals and different sidelobes between the original PWE and the FRF baseband data. Normalized cross-correlation coefficient at zero lag is calculated to quantify the degree of similarity at each imaging point and used as a weighting matrix to the FRF baseband data to further suppress sidelobes, thus improving the filter-retrieved focusing quality.

Keywords—retrospective synthetic focusing, high frame rate, correlation weighting.

I. INTRODUCTION

CONVENTIONAL ultrasound imaging systems employ fixed transmit focusing and dynamic receive focusing and thus multi-line electronic scanning is performed, resulting in 30 to 40-Hz frame rate. However, recently, a wide spectrum of new applications in biomedical ultrasound such as real time 3D ultrasound, vector velocity estimation, and transient elastography has triggered the need of high frame-rate imaging.

One of the methods to achieve high frame-rate imaging is to use plane wave excitation with which a single insonification is sufficient to form an image [1] [2]. Plane wave excitation (PWE) means all the transducer elements fire at the same time. With PWE, up to 5000 plane wave emissions per second are feasible; that is, high frame rate imaging with up to 5000-Hz frame rate is achievable. Recently, a serial of related researches have been launched [3]-[6]. However, due to the lack of transmit focusing, the signal-to-noise-ratio (SNR), contrast, and spatial resolution of the resultant images are hampered compared with a conventional focused transmission.

In this study, we proposed a filter-retrieved transmit focusing (FRF) technique along with correlation-coefficient weighting (FRF+CC weighting) to improve image quality of high frame-rate imaging with PWE. A 2D filter is designed to simultaneously minimize the predefined sidelobe energy associated with single PWE and the filter energy related to the SNR.

Chang-Lin Hu is with Industrial Technology Research Institute, Taiwan
e-mail:hulong@itri.org.tw

By adjusting the signal coherence of the beamformed PWE baseband data in the sliding filter kernel, this 2D filter attempts to maintain the mainlobe signals and to reduce the sidelobe ones. Thus, the mainlobe signals between the original PWE and the FRF baseband data will have high correlation while low signal correlation will be introduced for sidelobes [7]. Correlation coefficients (CC) between each imaging point in the PWE and the FRF images is therefore calculated [8] and then used as a weighting factor to further suppress sidelobes, thus improving the filter-retrieved focusing quality.

II. MATERIALS AND METHODS

The filter technique of retrospective transmitting focusing treats dynamic focusing as a deconvolution problem [8]. An SNR-dependent 2-D retrospective filter technique is employed in this study, which can improve both image quality and SNR along the range compared to 1-D lateral filtering. The 2D filter is derived from two point spread functions (PSFs): one PSF is the ideal PSF that is dynamic focusing on transmit and receive, and one PSF is the PWE PSF that is plane wave excitation on transmit and dynamic focusing on receive. The two PSFs give similar mainlobe signals and different sidelobe signals. The 2D filter is used to retain mainlobe and suppress sidelobe in PWE PSF. The 2D retrospective filter is defined as follows:

$$f_{OPT} = P^{-1} A_e^H A_e P^{-1} A_e^{-1} b_e \quad (1)$$

where $P = \alpha Q + \beta I$; α and β are the weightings and $\alpha + \beta = 1$; A_e is one of the row vector from “PWE PSF elements \times 2D filter elements convolution” matrix in which n-th row is the row-by-row reshaped version of the unfiltered PSF corresponding to n-th operation of the moving filter and be is set as unity [7].

The used 2D filter maintains the mainlobe signals and reduces the sidelobe ones by adjusting the signal coherence of the filter-coefficient weighted baseband data in the sliding filter kernel during the convolution sum, which is similar to the processing of phase rotation employed in baseband beamformers. For the mainlobe signals in the original PWE baseband data, in the sliding filter kernel, filter-coefficient weighted baseband data will pose high signal coherence, which results in constructive summation after the filter convolution sum and thus reinforces the mainlobe signals. On the other hand, for sidelobes, low signal coherence will be introduced, thus producing destructive interference and suppressing the sidelobes after the convolution sum, as shown in Fig.1 (a).

The mainlobe signals between the original PWE (Fig.1 (a)) and the FRF (Fig.1 (b)) baseband data will have high correlation while low signal correlation will be introduced for sidelobes. Correlation coefficients (CC) (Fig.1 (b)) between each imaging point in the PWE and the FRF images is therefore calculated and then used as a weighting factor to further suppress sidelobes, thus improving the filter-retrieved focusing quality (Fig.1 (c)).

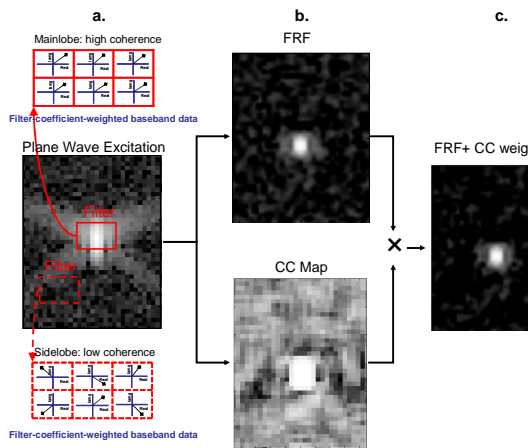


Fig. 1 Illustration of FRF+CC weighting technique

III. RESULTS AND DISCUSSION

Here simulations using Field II [9] were used to demonstrate the efficacy of the proposed FRF+CC weighting technique. A 128-element linear array with 5-MHz center frequency, 71% fractional bandwidth and 0.308-mm pitch was simulated. The F-number is set to 2 and the speed of sound is 1540 m/s in all the methods. There is no apodization on transmit and on receive. In the ideal focusing cases, multi-line scanning with dynamic transmit and receive focusing was performed with 64 active elements for each scan-line. Two phantoms – point targets and a cyst phantom were simulated. According to previous studies [6], the simulated SNR of the PWE cases was 18 dB lower than the ideal focusing one. In the simulation of two point targets, one of the two targets the back-scattering cross-section of one of the two targets is two times of that of the other. For the cyst phantom, there was an anechoic cyst with a 3-mm diameter centered at the depth of 30 mm. In the simulations, the lateral and axial filter size was selected as 30 and 8.5 wavelength at the imaging center frequency, respectively, and α is set to 0.5.

A. Point Target

Figs. 2(a)-(d) show the 50-dB B-mode images of the one point target with ideal focusing, plane wave excitation with dynamic receive focusing, the FRF technique, and the FRF+CC weighting technique, respectively. Although the FRF technique improves the quality of the PWE image, the sidelobe level is still high. The sidelobe level and mainlobe width of the FRF image are noticeably suppressed and narrowed by the CC weighting technique, as shown in Fig. 2(d). In addition, the background noise of the FRF PSF is suppressed after CC weighting.

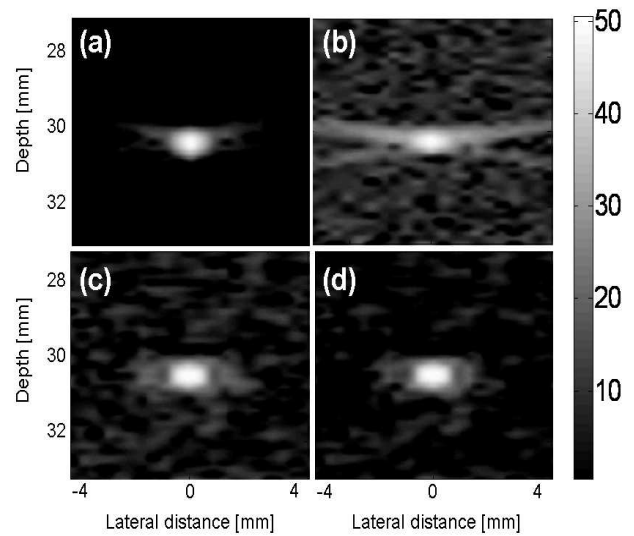
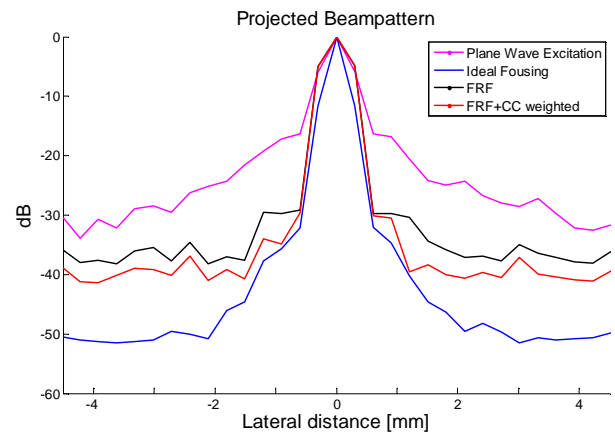


Fig. 2 50-dB B-mode images of the one point target with ideal focusing (a), plane wave excitation with dynamic receive focusing (b), the FRF technique (c), and FRF+CC weighting technique (d), respectively

Fig. 3 shows the projected lateral beam profiles of the images shown in Fig. 2. For ideal focusing, PWE, FRF technique, and FRF+CC weighting, the FRF technique can narrow mainlobe width and suppress sidelobe level by 10 dB, and then the FRF+CC weighting will further narrow mainlobe width and further suppress sidelobes by 5 dB. Thus, compared with PWE, the FRF+CC weighting technique can improve the mainlobe and also suppress sidelobes by 15 dB.



B. Anechoic Cyst

Figs. 4(a)-(d) show the 40-dB B-mode images of the simulated cyst phantom with ideal focusing, plane wave excitation with dynamic receive focusing, the FRF technique, and FRF+CC weighting, respectively. The CRs and CNRs were 34.58 dB and 7.74 for the ideal focusing image, 13.84 dB and 2.28 for PWE image, 23.38 dB and 4.84 for the FRF technique, and 33.98 dB and 6.30 for the FRF+CC weighting method. The CR and CNR improved by 9.54 dB and 112.28% with the FRF technique and by 20.14 dB and 176.32% with the FRF+CC weighting method.

The standard deviations in the speckle background were 4.47 dB for the ideal focusing image, 6.07 dB for PWE image, 4.83 dB for the FRF technique, and 5.39 dB for the FRF+CC weighting method. The FRF technique improves the quality of the PWE image, and furthers the FRF+CC weighted image shows a clearer anechoic region and enhanced discrimination of the internal architecture due to improvement of the contrast.

- [7] Chang-Lin. Hu, Geng-Shi. Jeng, Yu-Hsin. Wang, Pai-Chi. Li, and Meng-Lin. Li, Improved Plane-Wave High Frame Rate Imaging Using Retrospective Transmit Focusing and Filter-derived Coherence-Index Weighting. in Proc. IEEE Ultrason. Symp., 2010.
- [8] Chi Hyung. Seo and Jesse T. Yen, Sidelobe Suppression in Ultrasound Imaging using Dual Apodization with Cross-correlation. IEEE Trans. Ultras., Ferro., And Freq. Control., 55(10), 2198-2210, 2008
- [9] J. A. Jensen, "Field: A program for simulating ultrasound systems," Medical & Biological Engineering & Computing, vol. 34, pp. 351-353, 1996.

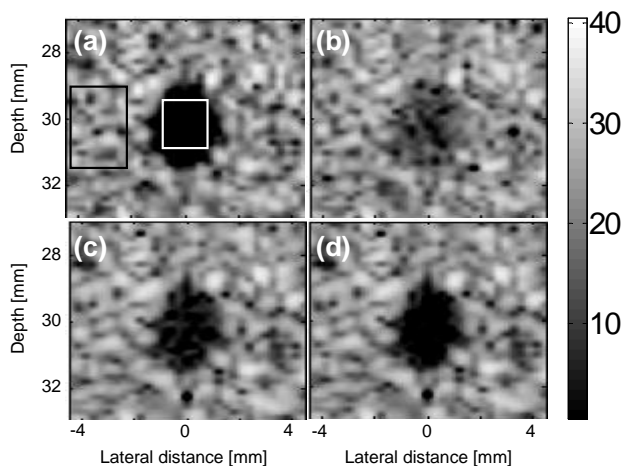


Fig. 4 40-dB B-mode images of the simulated cyst phantom with ideal focusing (a), plane wave excitation with dynamic receive focusing (b), the FRF technique (c), and FRF+CC weighting (d)

IV. CONCLUSIONS

From our simulation, it is shown that the FRF+CC weighting technique can improve the image quality of high frame-rate imaging with single PWE – suppressing the sidelobes and improving the SNR while retaining the frame rate. Because of only beamformed baseband data being required and high frame rate nature of PWE, the proposed technique owns low computational complexity and is inherently unsusceptible to motion artifacts.

REFERENCES

- [1] B. Delannoy, R. Torgue, C. Bruneel, and E. Bridou, "Ultrafast electronical image reconstruction device" in Echocardiology, vol. 1, C. T. Lancee, Ed. (The Hague: Nijhoff, 1979), ch. 3, pp. 447-450.
- [2] B. Delannoy, R. Torgue, C. Bruneel, E. Bridoux, J. M. Rouvaen, and H. LaSota, "Acoustical image reconstruction in parallel-processing analog electronic systems," J. Appl. Phys., vol. 50, pp. 3153-3159, May 1979.
- [3] Shattuck, D., Weinshenker, M., Smith, S., and Ramm, O.V., "Explososcan: a parallel processing technique for high speed ultrasound imaging with linear phased arrays," J. Acoust. Soc. Am., vol. 75, no. 4, pp. 1273-1282, 1984.
- [4] Tanter, M., Bercoff, J., Sandrin, L., and Fink, M., "Ultrafast Compound Imaging for 2-D Motion Vector Estimation: Application to Transient Elastography," IEEE transactions on ultrasonics, ferroelectrics, and frequency control, vol. 4, no. 10, pp. 1363-1374, 2002.
- [5] Jesper Udesen, F.G., Kristoffer Lindskov Hansen, Jorgen Arendt Jensen, Carsten Thomsen, and Michael Bachmann Nielsen, "High Frame-Rate Blood Vector Velocity Imaging Using Plane Waves: Simulations and Preliminary Experiments," IEEE transactions on ultrasonics, ferroelectrics, and frequency control, vol. 55, no. 8, pp. 1729-1743, 2008.
- [6] Montaldo, G., Tanter, M., Bercoff, J., Benech, n., and Fink, M., "Coherent Plane-Wave Compounding for Very High Frame Rate Ultrasonography and Transient Elastography," IEEE transactions on ultrasonics, ferroelectrics, and frequency control, vol. 56, no. 3, pp. 489-506, 2009.